Theoretical and Applied Climatology (2024) 155:85–104
https://doi.org/10.1007/s00704-023-04587-x

RESEARCH

Flash drought evaluation using evaporative stress and evaporative demand drought indices: a case study from Awash River Basin (ARB), Ethiopia

Yitea Seneshaw Getahun[1] · **Ming-Hsu Li**[2]

Received: 4 August 2022 / Accepted: 2 August 2023 / Published online: 14 August 2023

Abstract

Drought is one of the most devastating phenomena that affect the livelihood of most communities in Ethiopia as they have low adaptive capacity. Recent advancements in remote sensing and drought investigations have made it possible to identify a new type of flash drought that has rapid intensification with a short duration (i.e., less than 1 month unlike conventional droughts). This study intends to identify flash drought in the Awash River Basin (ARB) based on Moderate Resolution Imaging Spectroradiometer (MODIS) data of actual evapotranspiration and potential evapotranspiration using Evaporative Demand Drought Index (EDDI) and Evaporative Stress Index (ESI) indices. The flash drought result exhibited that agricultural lands, grasslands, vegetation areas, and irrigational croplands along the river were vulnerable to flash drought in the ARB. Using ESI, the area of ARB that experienced flash drought in 2002, 2008, 2009, 2012, and 2015 were 23%, 40%, 20%, 40%, and 24%, respectively. These intense flash drought areas can be used as drought monitoring sites. The flash drought extent of EDDI is more compared to ESI because of ESI's dependency on vegetation coverages and soil moisture. The lowland downstream part of the ARB is highly prone to flash drought, particularly in the major rainy season (MRS) and the last two months of the minor rainy season (mRS). EDDI can discern the onset of flash drought better compared to ESI, but both can be used as a drought early warning mechanisms to minimize agricultural losses and drought-associated risks in the basin.

1 Introduction

Drought is a complex climate extreme phenomenon mostly caused by a prolonged period of rainfall deficit (meteorological drought) followed by soil moisture deficit, which in turn leads to a loss of streamflow and water shortage (Wilhite 2002; Van Loon 2015; Wilhite and Pulwarty 2017). It is one of the most devastating natural disasters due to its consequence on agricultural activities and water resources and has resulted in severe economic, environmental, and societal problems worldwide. Past studies have indicated that Ethiopia has been plagued by frequent, severe, long-lasting, and catastrophic droughts that influence the lives of millions of people through crop failure, water shortage, conflict, epidemics outbreaks, and death of human and livestock (Mera 2018; Gebremeskel et al. 2019). For instance, in 2008 alone about 26000 livestock were lost in Borena district only, 14 million people were affected and the cost of humanitarian aid was estimated to be $1077.8 million (World Bank 2017; Mohammed et al. 2017). In recent years, the frequency and severity of droughts have increased in Ethiopia, which resulted in huge economic losses in 2002,

Highlights
- Flash drought identification is essential for drought early warning and monitoring.
- EDDI's identification of a flash drought is more extensive than ESI's.
- Agropastoralists in the downstream basin were particularly vulnerable to flash droughts.
- Areas of grassland were hotspots for severe flash drought that can be used as monitoring sites.

✉ Yitea Seneshaw Getahun
yiseneshaw@dbu.edu.et

Ming-Hsu Li
mli@ncu.edu.tw

[1] College of Agriculture and Natural Resource Sciences, Department of Natural Resources Management, Debre Berhan University, P.O.Box 445, Debre Berhan, Ethiopia

[2] Graduate Institute of Hydrological and Oceanic Sciences, National Central University, 320 Taoyuan, Taiwan

2003, 2004, 2005, 2006, 2008, 2009, 2011, 2012, 2015, and 2016 (MacDonald et al. 2019; Liou and Mulualem 2019; USAID 2018; Suryabhagavan 2017; El Kenawy et al. 2016; Masih et al. 2014; Mays 2014; Viste and Sorteberg 2013). These recent increases in drought severity and frequency in Ethiopia may be highly associated with global warming (Mera 2018; El Kenawy et al. 2016).

Conventional droughts are generally slowly developing and receding phenomena with various longevity causing substantial socioeconomic impacts as their most common characteristics (Wilhite and Pulwarty 2017; Svoboda et al. 2002; Wilhite 2002). However, current studies have revealed a new type of flash drought, which has been defined based on its rapid rate of intensification (Ford and Labosier 2017; Ford et al. 2015) or short duration from days to weeks due to atmospheric anomalies of rainfall deficit and high temperature that may further lead to soil moisture deficit (Yao et al. 2018; Zhang et al. 2019; Mo and Lettenmaier 2016; Hobbins et al. 2016; McEvoy et al. 2016; Otkin et al. 2014). Otkin et al. (2018), which has distinct characteristics, unlike conventional drought properties of long-lastingness. According to Otkin et al. (2018), flash drought can be identified based on its rapid rate of intensification (i.e., flash part) and moisture limitation (i.e., drought part). The onset and propagation of flash drought can occur rapidly when atmospheric anomalies such as rainfall deficit and high temperatures persist for several weeks (Christian et al. 2019a, 2019b; Svoboda et al. 2002). Flash drought has been largely affecting crop yields, water resources, natural ecosystems, and soil moisture (Christian et al. 2019a, 2019b). Flash droughts can be easily intensified by human-induced climate change or increasing temperature and monitoring flash drought is indispensable to developing drought early warning systems that can minimize agricultural and economic losses. Detecting and monitoring the likely occurrences of flash and long-lasting droughts can help to minimize the disastrous impacts of droughts. Flash drought evaluations should be incorporated into conventional drought monitoring programs for early warning and proactive measures to lessen the overall drought risk.

High rainfall variability and low adaptation capacity have been the main challenge in Ethiopia, which impacts agricultural productivity causing severe food security problems in the entire country (Gebissa and Geremew 2022). Improving climate extreme analysis and climate information/services for smallholder farmers are essential to increase agricultural production with effective adaptation strategies against extreme events. However, studies that quantify climate risks and provide climate services with adaptation strategies for smallholder farmers are very limited in Ethiopia. Without climate information to support drought watch, various extents, frequencies, and severities of droughts have caused great socioeconomic impacts on the livelihood of the ARB. Recent developments in remote sensing and drought research have shown possibilities to identify a new type of flash drought that has rapid intensification within a short duration (e.g., days, weeks) unlike the conventional drought lasting longer than one month. Since EDDI and ESI indices are highly sensitive to climate variables (e.g., temperature and rainfall), they can be applied to access climate change impacts and also serve as precursors for conventional droughts by detecting flash droughts. Therefore, characterizing and identifying flash drought areas with EDDI and ESI have the advantages to provide valuable information for climate services and adaptation decision-making. For example, flash drought hotspots can be identified by both indices as vulnerable areas for drought impacts and require considerations for deploying monitoring instruments to detect the onset of future droughts. Smallholder farmers in the ARB are aware of increasing temperatures and the anomalous nature of rainfall, as well as their agricultural activities and productions have been compromised by frequent droughts. Considering drought in changing climate that may increase risks of food security in the ARB, developments of adaptation pathways should be informed with quantitative drought extents, frequencies, and severities. In addition, drought-monitoring instruments should be deployed in flash drought-prone areas to detect drought onset and to support predictions of drought longevity.

Droughts have been frequent and catastrophic in the Great Rift Valley, eastern, and southeastern parts of Ethiopia, where the Awash River basin (ARB) is located (Thomas et al. 2019; Mera 2018; Shiferaw et al. 2014). The ARB is the most populated and utilized basin in the country, which has been seriously affected by water scarcity and recurring droughts causing problems with food security (Hailu et al. 2017; Adeba et al. 2015; Edossa et al. 2010; Murendo et al. 2010). In recent years, better understanding, identification, and monitoring of droughts have been available by utilizing new technological advancements such as remote sensing products and drought indices (Yu et al. 2019; Christian et al. 2019a, 2019b; Otkin et al. 2018). Satellite datasets are cost-effective, vital in areas where ground-based datasets are not adequate, and important to provide better spatial information relative to observed data that requires interpolation (Sun et al. 2018; AghaKouchak et al. 2015). Therefore, monitoring and identifying flash drought using advancements in remote sensing outputs and newly developed flash drought indices is vital for the improvement of agricultural productivity.

Studies in Ethiopia or ARB have been mostly analyzing conventional droughts using indexes like SPI, VCI, and NDVI with rather less attention on the rapidly evolving flash droughts (MacDonald et al. 2019; Mera 2018; Suryabhagavan 2017; Edossa et al. 2010). Moreover, the effect of global warming was not well characterized by most of the previous drought indices. Recently, new drought indices

have been proposed with information on atmospheric water demand or increasing temperature. Among those new indices, both Evaporative Demand Drought Index (EDDI) and Evaporative Stress Index (ESI) are highly sensitive to several climate variables including temperature, rainfall, and soil moisture, which are important to characterize rapidly evolving drought events (Pendergrass et al. 2020; McEvoy et al. 2016; Otkin et al. 2014; Vicente-Serrano et al. 2010). In this study, we aim to identify flash drought using both ESI and EDDI drought indices. The commonly used drought index of Standardized Precipitation Index (SPI) calculated with rainfall data will be compared with both ESI and EDDI to examine whether the satellite data is applicable to better characterize drought in the basin or not. The objectives of this study include (1) validating the satellite output with SPI and evaluating flash drought in ARB using ESI and EDDI drought indices; (2) examining flash drought intensity; and (3) identifying flash drought hotspot areas in the basin. For the sake of clarity and to read it easily, dominantly used abbreviations are presented in Table 1.

2 Dataset and methods

2.1 Study area

The ARB lies in the east-central part of Ethiopia between 7°52′–12°N and 37°57′–43°25′ E as shown in Fig. 1a. The Awash River has a length of 1200 km and a basin area of about 116,374 km^2 with an irrigation potential of 205,400 hectares (Dost et al. 2013). The elevation of ARB ranges from 215 to 4185 m with the Awash River originating from the central highlands and meeting the Red Sea at Lake Abbe near Djibouti (Fig. 1b). About 24 million population (18 M people and 6 M livestock) are assessed to live in the ARB along with the major industries in big cities including the

Table 1 Abbreviation

Abbreviation	Full name	Abbreviation	Full name
ARB	Awash River Basin	EDDI	Evaporative Demand Drought Index
MODIS	Moderate Resolution Imaging Spectroradiometer	ESI	Evaporative Stress Index
AET	Actual evapotranspiration	SPI	Standardized Precipitation Index
PET	Potential evapotranspiration	MRS	Major rainy season, Jun-Sep (JJAS),
mRS	Minor rainy season, Feb–May (FMAM)		

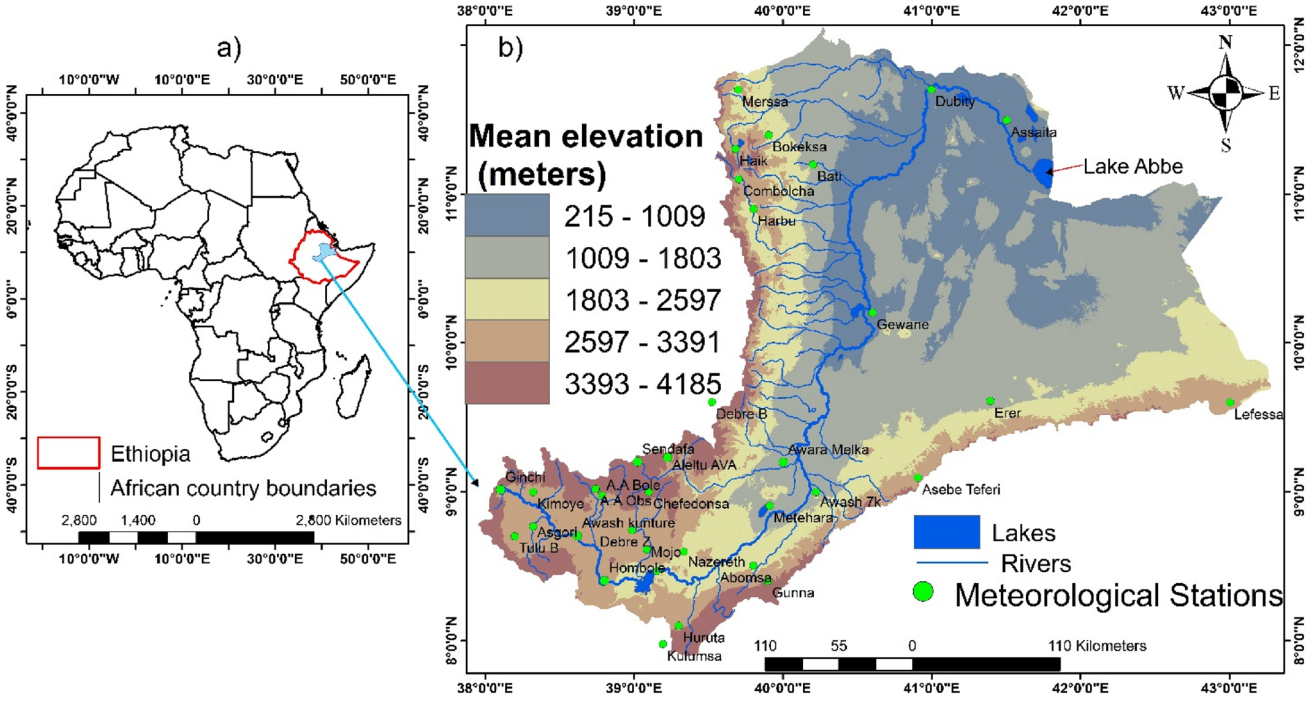

Figure 1 Study area location map: **a** Africa, Ethiopia, ARB; **b** Meteorological stations, Lakes, mean elevation, major rivers in the ARB

capital city of Addis Ababa, which makes the ARB the most utilized basin in the country (Hailu et al. 2017).

Due to distinct seasonal rainfall amounts, the ARB has three seasons: (i) the main rainy season (MRS), nationally called "Kiremt" from Jun-Sep (JJAS), (ii) the minor rainy season (mRS), nationally known as "Belg" from Feb-May (FMAM), and (iii) the dry season, also called "Bega" from Oct to Jan (ONDJ) (Degefu et al. 2017). In addition to the rotation of the Earth around the sun, the monsoon system, and atmospheric circulation, the rugged topography also plays a significant role in affecting regional rainfall distribution (Viste 2012).

As indicated in Fig. 2, based on data from 1986 to 2016, the mean annual rainfall in the upstream and northwestern peripheries of the basin is relatively high that varies from varies from 900 to 1300 mm. Similarly, the major rainy season rainfall is also comparatively high in the upstream and northwestern peripheries of the basin that varies from 620 to 930 mm, whereas the minor rainy exhibited high rainfall in the northwest and southern peripheries of the basin. The highest monthly rainfall is indicated in July and August which is about 200 mm. The highest rainfall in most of the areas and seasons are associated with elevation and high elevated areas showed high rainfall compared to the lowland areas.

2.2 Data

2.2.1 MODIS data

The potential evapotranspiration (PET) and actual evapotranspiration (AET) data measured by the Moderate Resolution Imaging Spectroradiometer (MODIS) aboard the Terra satellite of the National Aeronautics Space

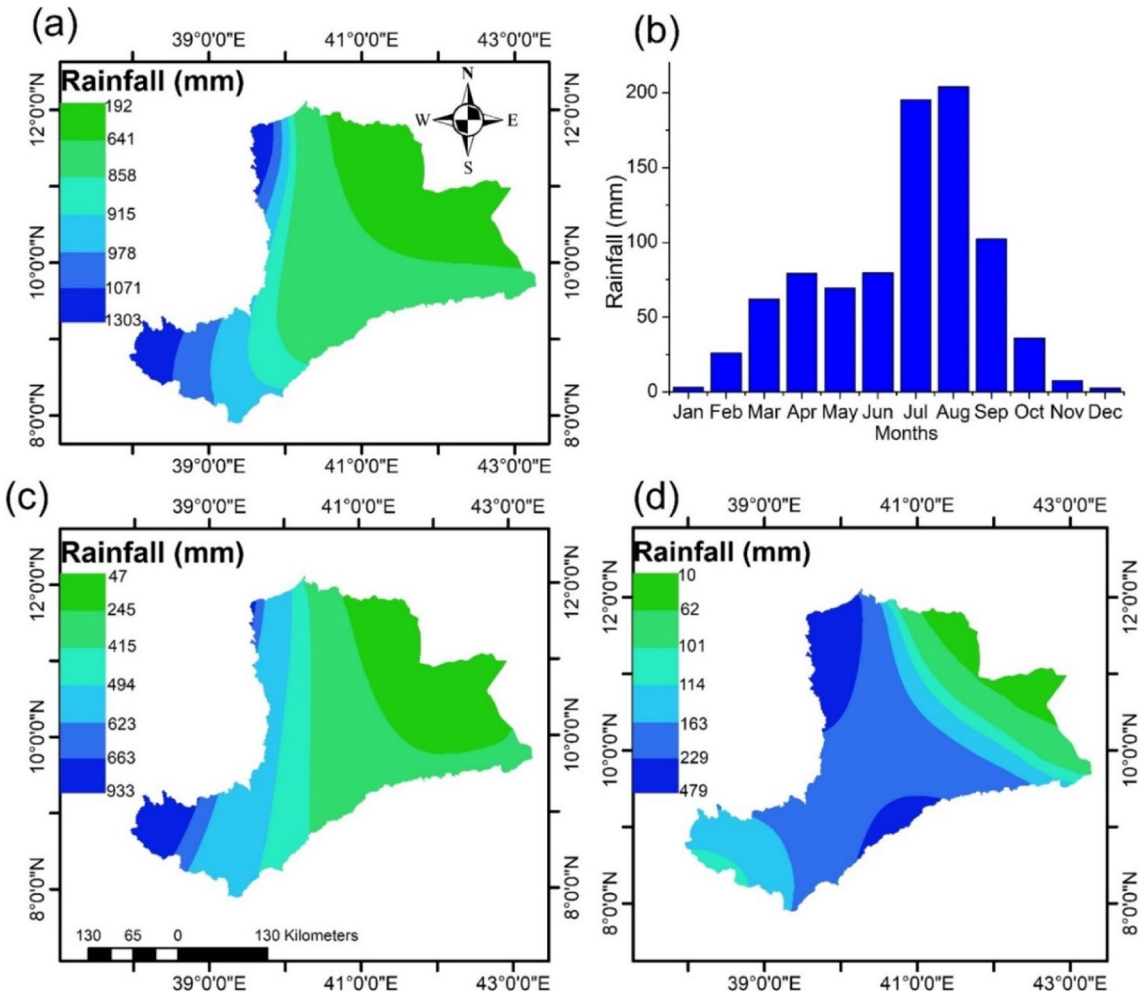

Figure 2 Spatial average annual and seasonal rainfall distribution of ARB (from 1986 to 2016): **a** annual rainfall, **b** average monthly rainfall, **c** major rainy season rainfall, and **d** minor rainy season rainfall

Administration (NASA) were obtained from the United States Geological Survey (USGS) web service (https://e4ftl01.cr.usgs.gov/MOLT/MOD16A2.006/). The MODIS Terra dataset of MOD16A2 with an 8-day temporal scale (8-day average) was used in this study with a spatial resolution of 500 m (Running et al. 2017a, 2017b). The downloaded .TIF format data was processed using R and ArcGIS software. The AET and PET data used for this study were obtained from 2002-2017. The MOD16A2 product of AET was computed using the Penman-Monteith equation, while the Priestley–Taylor equation was used to calculate the PET (Mu et al. 2007; Mu et al. 2011). The detailed flow chart for generating AET and PET products of MOD16A2 can be found in the MODIS user's guide (Running et al. 2017a, 2017b; Priestley and Taylor 1972).

2.2.2 Observed meteorological datasets

The observed rainfall data for 15 years (2002–2016) were obtained from 35 stations of the National Meteorological Institute (NMI), Ethiopia (Fig. 2). The data obtained from NMI were preprocessed and quality-checked.

2.3 Flash Drought Indices

2.3.1 Evaporative Stress Index

Based on the definition of flash drought given by Otkin et al. (2018), a methodology of characterizing flash drought suggested by Christian et al. (2019a, 2019b) was adopted in this study (Fig. 3). Unlike slow-developing conventional droughts to be examined in monthly or longer time scales, flash drought investigation should be carried out in shorter time scales such as daily and weekly. Drought indices of the Evaporative Stress Index (ESI) and EDDI were used to identify flash drought based on the MODIS Terra products of average weekly AET and PET in this study. The MODIS data were processed from 2002 to 2017 with flash drought analysis carried out in selected recent drought years.

The ESI is computed as a ratio of AET to PET (Anderson et al. 2016; Sur et al. 2015; Anderson et al. 2011). It is defined as

$$ESI = \frac{AET}{PET} \tag{1}$$

The ESI is further standardized to be the Standardized ESI (SESI) computed as

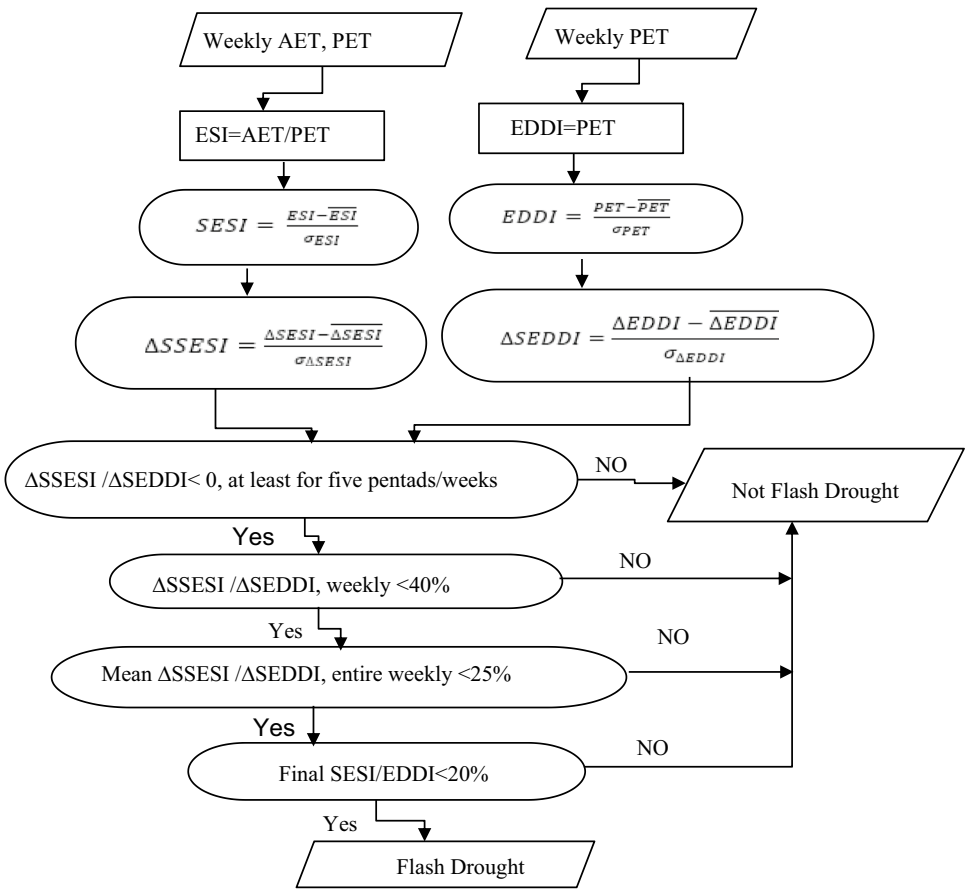

Figure 3 General methodology of flash drought based on ESI and EDDI

$$SESI = \frac{ESI - \overline{ESI}}{\sigma_{ESI}} \quad (2)$$

where the $\overline{ESI}$ and the σ_{ESI} stands for the average and the standard deviation of ESI, respectively, for the whole study period from 2002 to 2017. In practice, standardization is a useful process for a more easy and robust comparison of different climatic regimes and growing seasons over multiple years (Christian et al. 2019a, 2019b).

Additionally, the standardized ESI change (ΔSSESI) anomalies were computed over selected weeks:

$$\Delta SSESI = \frac{\Delta SESI - \overline{\Delta SESI}}{\sigma_{\Delta SESI}} \quad (3)$$

where the ΔSSESI is the standardized change in SESI, the Δ*S*ESI is the change in SESI, the $\overline{\Delta SESI}$ is the average change in SESI for the entire period investigated in this study and the $\sigma_{\Delta SESI}$ is the standard deviation of the SESI considering all available years in the dataset.

The ESI is sensitive to moisture stress that indicates terrestrial water availability (Zhang et al. 2019). The ESI value ranges from zero to one that is associated with dryness or wetness conditions of the land surface. The larger (positive) ESI means the atmospheric demand of evapotranspiration is well fulfilled by vegetation and existing soil moisture, whereas the lower (negative) means the land surface hardly fulfilled any of the atmospheric evaporative demand (Christian et al. 2019a, 2019b). The positive ESI value indicates less or no drought occurrence, whereas the negative ESI value shows the occurrence of drought for a given location and period (McEvoy et al. 2016). Normalization by PET helps to minimize the AET variation due to the seasonal difference of available energy as well as vegetation coverage, which provides weightage to currently available moisture for the vegetation regardless of previous moisture conditions (Farahmand 2016; Anderson et al. 2016).

2.3.2 Evaporative Demand Drought Index

The Evaporative Demand Drought Index (EDDI) is a newly proposed drought index that only relies on potential evapotranspiration (PET) (Hobbins et al. 2016). It measures the drying potential of the atmosphere that induces vegetation stress on the ground (McEvoy et al. 2019). In other words, it is used to monitor the atmospheric evaporative demand that leads to the onset and development of droughts when extreme atmospheric anomalies like high temperature or rainfall deficits persist for several weeks (Christian et al. 2019a, 2019b). EDDI is a useful index to indicate rapidly evolving (developing over a few weeks) and sustained (months or years) drought events (Hobbins et al. 2016). It is highly recommended for flash drought analysis because of its inter-dependency on rainfall, soil moisture, and topography (McEvoy et al. 2019). Moreover, recent studies have shown that places around the world have been experiencing more frequent drought because of the rising global temperature (Ford et al. 2015; Otkin et al. 2014; Zhang et al. 2019). EDDI can easily indicate the early onset and development of rapid drying conditions prior to other indicators namely, rainfall, soil moisture, and AET (McEvoy et al. 2019). First, PET was standardized like that of SESI, which is computed as follows (Hobbins et al. 2016):

$$EDDI = \frac{PET - \overline{PET}}{\sigma_{PET}} \quad (4)$$

where EDDI represents standardized PET, PET represents the potential evapotranspiration on a weekly time scale, $\overline{PET}$ is the long-term mean of weekly PET from 2002 to 2017 and σ_{PET} is the standard deviation of long-term PET. Secondly, the standardized PET (EDDI) change anomalies were computed over specific weekly intervals:

$$\Delta SEDDI = \frac{\Delta EDDI - \overline{\Delta EDDI}}{\sigma_{\Delta EDDI}} \quad (5)$$

where, ΔSEDDI is the standardized change in EDDI, ΔEDDI is the change in EDDI, $\overline{\Delta EDDI}$ is the average change in EDDI for all years available in the dataset, and $\sigma_{\Delta EDDI}$ denotes the standard deviation of EDDI for all years available in the dataset.

Based on the approach proposed by Christian et al. (2019a, 2019b), a flash drought phenomenon is identified to have (1) a minimal length of five negative SESI /EDDI changes, correspondent to a length of six weeks (i.e., 30 days), (2) a final SESI/EDDI value below the 20th percentile from the average SESI/EDDI, (3) week-to-week changes in SSESI/SEDDI must be below the 40th percentile between individual weeks, and (4) the mean changes in SSESI/ SEDDI must be below the 25th percentile for the entire weeks. It is noted weeks are equal to pentads in their approach. The earlier two criteria focus on drought impacts on vegetation related to soil moisture depletion that fulfills the drought component, whereas the final two focus on the speedy intensification to fulfill the flash component of drought (Christian et al. 2019a, 2019b). A minimum of six pentads were suggested to smooth out the short-term fluctuation in SESI/EDDI and to eliminate the short-term dry spells. The SESI/EDDI value below the average for a longer period of time that is below the 20th percentile threshold fulfill the drought component. The third criterion (40th percentile) threshold is less strict and it is used to isolate deteriorating conditions (< 40th percentile) from that of improving conditions (>40th

percentile) in individual pentads. Moreover, it is possible that some weeks in SESI/EDDI will exhibit very quick development, whereas others will experience slower intensification. However, these issues in the third criterion can be corrected by the average change in SSESI/SEDDI must be below the 25th percentile during the flash drought event (Christian et al. 2019a, 2019b).

2.3.3 Standardized Precipitation Index (SPI)

The Standardized Precipitation Index (SPI) index proposed by McKee et al. (1993) to characterize rainfall deficit in multiple time scales was used to detect drought for different areas (Munagapati et al. 2018). Several studies in Ethiopia have used the SPI to evaluate meteorological droughts (Teweldebirhan et al. 2019; Suryabhagavan 2017; Zeleke et al. 2017; Viste and Sorteberg 2013). Since SPI is normalized to the required location with various time scales, it is commonly accepted and applied worldwide for different applications (Masih et al. 2014). The SPI is not only flexible but also solely requires rainfall data making it suitable for complex topography and climatic regions (El Kenawy et al. 2016). The standardized or normalized average monthly rainfall data obtained from 35 meteorological stations of the ARB was used to compute the SPI values and then compared with MODIS-based ESI and EDDI drought indices for verification. Correlations between the SPI and the ESI and the EDDI were evaluated to check how the ESI and EDDI indices obtained from the MODIS data were capable to characterize droughts in the basin.

As shown in Table 2, the EDDI, SPI, and ESI drought severity classes were scaled on constant and equal ranges. These drought severity classes are used to describe the extent or magnitude of drought events over the ARB.

Table 2 Drought severity classes of drought indices values (McKee et al. 1993)

Drought condition		SPI / ESI/ EDDI
Extreme drought		≤ −2
Severe drought		−1.5 to −1.99
Moderate drought		−1.0 to −1.49
Near normal	Mild drought	−.99 to −0.5
	Normal	−0.5 ≤0 ≤ 0.5
	Mild wet	0.5 to .99
Moderate wet		1.0 to 1.49
Very wet		1.5 to 1.99
Extremely wet		≥2.0

3 Results and discussion

3.1 Pattern of AET and PET in Awash River Basin

Figure 4 presents the spatial distribution of monthly average AET and PET in the ARB using MODIS products from 2002 to 2017. High monthly average AET that varied in a range of 0.5 to 5 mm/day was observed in the upstream, northwest, and southwest peripheries of the basin with a high basin area of 58.5% (68085.7 km^2) in August and reduced to the coverage area of about 31.6% (35253.2 km^2) in February (Fig. 4a). On the other hand, the AET in the downstream (semi-arid to arid) part of the basin had a range of 0 mm/day to 0.5 mm/day for a high basin area of 57.5 % (66923.3 km^2) in February, while it was low in August covering 27.9% (32473.3 km^2) of the basin area. Specifically, the highest monthly average AET in a range of 3 to 5 mm/day was observed in the forested and shrub-lands of the upstream basin with coverages of 2934.4 km^2 in September and 881.6 km^2 in August and the lowest coverage in March (74.5 km^2). The AET in a range of 1.5 to 5 mm/day was high in August, September, and October and covered 33.8% (39380.9 km^2), 32.4% (37700.5 km^2), and 19.8% (23029.1 km^2) of the basin area, respectively, and it had the lowest coverage of 3% (3095.5 km^2) in March. Because of the sufficient rainfall in the MRS, the growth of agricultural crops and natural vegetation cover in the upstream, northwest, and southwest peripheries of the basin, which explain the larger monthly AET as compared to the downstream part of mostly arid or semi-arid bare land with inadequate rainfall. In most of the basin, the lowest AET range of 0 to 1 mm/day was observed in December, January, and February months. The spatial pattern of AET in the ARB is highly correlated with the spatial patterns of rainfall such that the elevated and high rainfall (humid) area of the basin shows the highest AET relative to the downstream low rainfall (arid, semi-arid) part of the basin.

As shown in Fig. 4b, the spatial pattern of PET is contrary to that of AET such that the highest PET is exhibited in the downstream or central part of the basin and the lowest PET is shown in the upstream part of the basin. The spatial pattern of PET corresponds to the temperature pattern, while the AET pattern resembles rainfall. The monthly spatial PET of the entire basin was in the range of 2 to 10.5 mm/day. The lowest PET range of 2 to 4.5 mm/day was exhibited in June, July, August, and September with a basin area of 212.7 km^2, 9316.6 km^2, 5449.3 km^2, and 258 km^2, respectively, which mainly occurred in the upstream basin (i.e., low temperature due to high elevation) during the MRS (i.e., high rainfall). The highest PET with a range of 9.5 to 10.5 mm/day occurred in May and

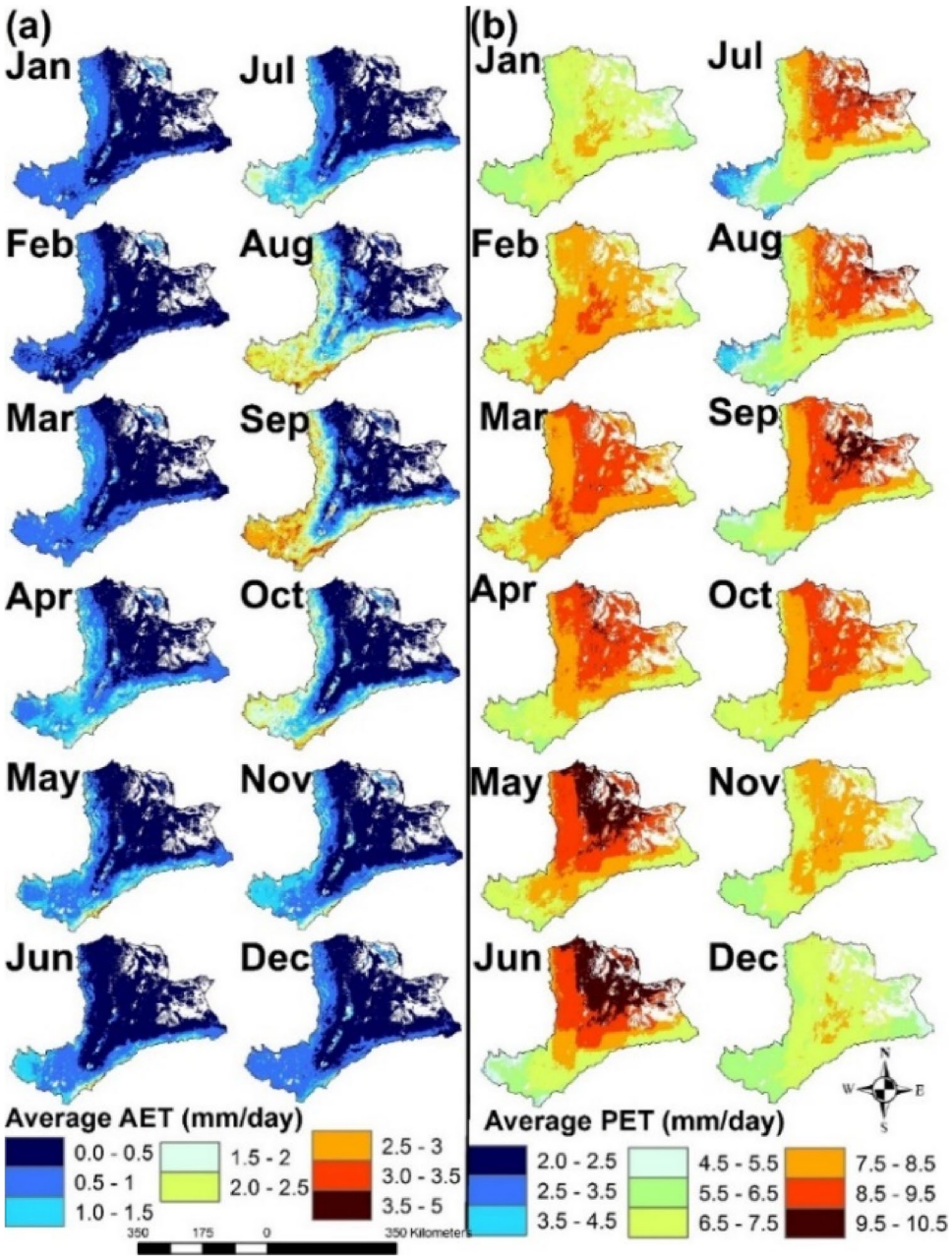

Figure 4 Monthly actual evapotranspiration (**a**) and potential evapotranspiration (**b**) of ARB from 2002 to 2017

June mainly found in the downstream basin covering 17.4 % (20299.2 km^2) and 21.9 % (25492.7 km^2) of the basin. Afterwards, the PET range of 8.5 to 9.5 mm/day occurred in March, April, May, September, and October with the basin area of 31.9 % (37131.7 km^2), 31.4 % (36573.6 km^2), 29.9 % (34818.5 km^2), 27.3 % (31732.1km^2), and 26.2 % (30532.6 km^2), respectively. Overall, the highest PET occurred in the downstream basin mainly covered by rangeland (grassland). Similar to those observed in AET, the lowest PET occurred in December and January due to the lowest temperature throughout the entire basin. It is noted the white color in the spatial map without AET and PET values were caused by urban areas, barren lands, sparse vegetation (rock, tundra, desert), and cloud coverage of MODIS satellite images.

3.2 SPI comparison with ESI and EDDI

The most widely used SPI drought index was computed using the basin average rainfall from 35 meteorological stations. The basin monthly average AET and PET were used to generate ESI and EDDI indices. As explained in the previous section, both AET and PET were highly affected by seasonal rainfall. It is expected that ESI and EDDI will highly correlate to the SPI. The time series of EDDI, ESI, and SPI were shown in Fig. 5. The result

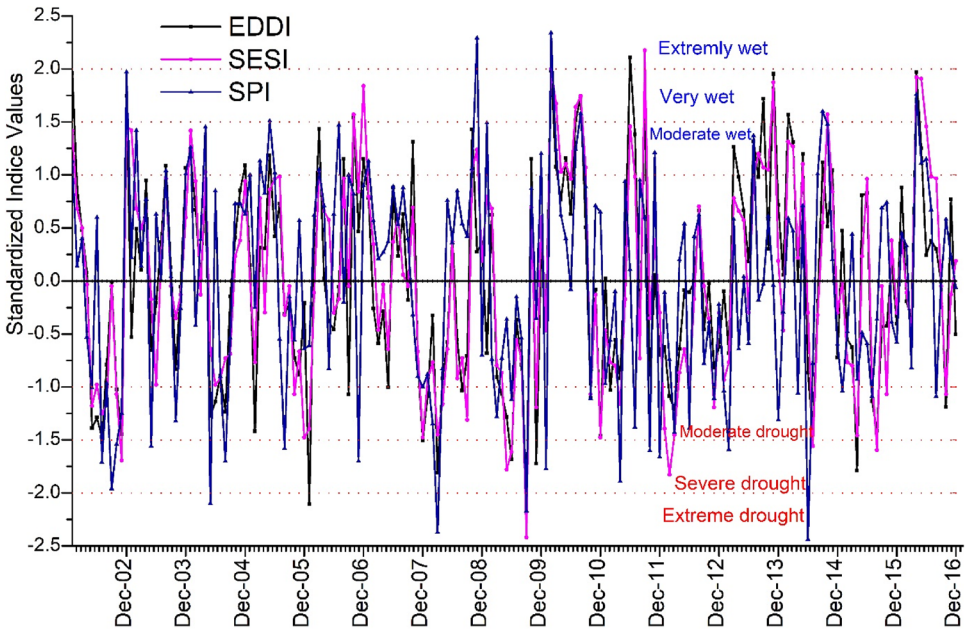

Figure 5 Comparison of monthly based drought indices of EDDI, SESI, and SPI

showed that the three indices were quite consistent with each other to capture the most extreme, severe, and moderate drought years, as well as the wet years. The SPI correlation with EDDI and ESI were 0.76 and 0.79, respectively, which implies that the MODIS satellite products are suitable for characterizing dry and wet conditions in the ARB. The correlation between EDDI and ESI was 0.89. Considering monthly time series were used in this study, the number of drought events might increase with a shorter time resolution as the indices (e.g., SPI, ESI, and EDDI) quickly changed between wet and dry months. However, the most devastating drought years were 2000, 2004, 2005, and 2006. 2008, 2009, and 2012.

3.3 Evaluating flash drought using ESI and EDDI

The shorter duration of weekly ESI and EDDI can indicate the early onset of drought that cannot be detected by conventional drought analysis with monthly data. Flash drought in the ARB was examined during the two growing seasons of the mRS (Feb–May) and the MRS (June–Sep) because the evaporative stress is less sensitive to drought in non-growing seasons (Christian et al. 2019a, 2019b). Recent historical drought years of 2002, 2008, 2009, 2012, and 2015 were used to evaluate the spread of flash drought over the ARB. Figures 6 and 7 showed the spatial evolution of flash drought in 2008 historical drought, which were results of flash drought areas identified by weekly ESI and EDDI drought indices and followed the criteria of flash drought as mentioned in Christian et al. (2019a, 2019b).

3.3.1 ESI-based evolution of 2008 flash drought

The distributions of flash drought in 2008 mRS and MRS with weekly ESI were depicted in Figs. 6a and 6b, respectively. The flash drought in 2008 mRS started in the second week of February in the upstream basin and expanded to the northwestern and southwestern peripheries and along with the river (Fig. 5a). The downstream part of ARB experienced less flash drought in February and March. During April and May, the flash drought over the upstream basin has become less and shifted to the downstream part, particularly the northeastern and southeastern basins. However, the flash drought extent varied quickly from one week to another. The upstream basin experienced flash drought during the first two months of mRS. It is noted the area along the river was vulnerable to flash drought throughout the entire mRS due to the presence of better vegetation coverage and high temperature. The shift of flash drought in April and May might be caused by the erratic minor rainfall started in the downstream basin to trigger the grassland to grow. Figure 6b presented the spread of flash drought during the MRS. Unlike the spatial shifts of flash drought observed in 2008 mRS (Fig. 5a), the downstream basin was mainly identified to experience flash drought during the MRS. Moreover, the flash drought in the MRS extended in June and the first week of July was larger than that of other weeks.

3.3.2 EDDI-based evolution of 2008 flash drought

The spread of flash drought in 2008 mRS and MRS with weekly EDDI were depicted in Figs. 7a and 7b, respectively. Similar to the ESI results, the EDDI results

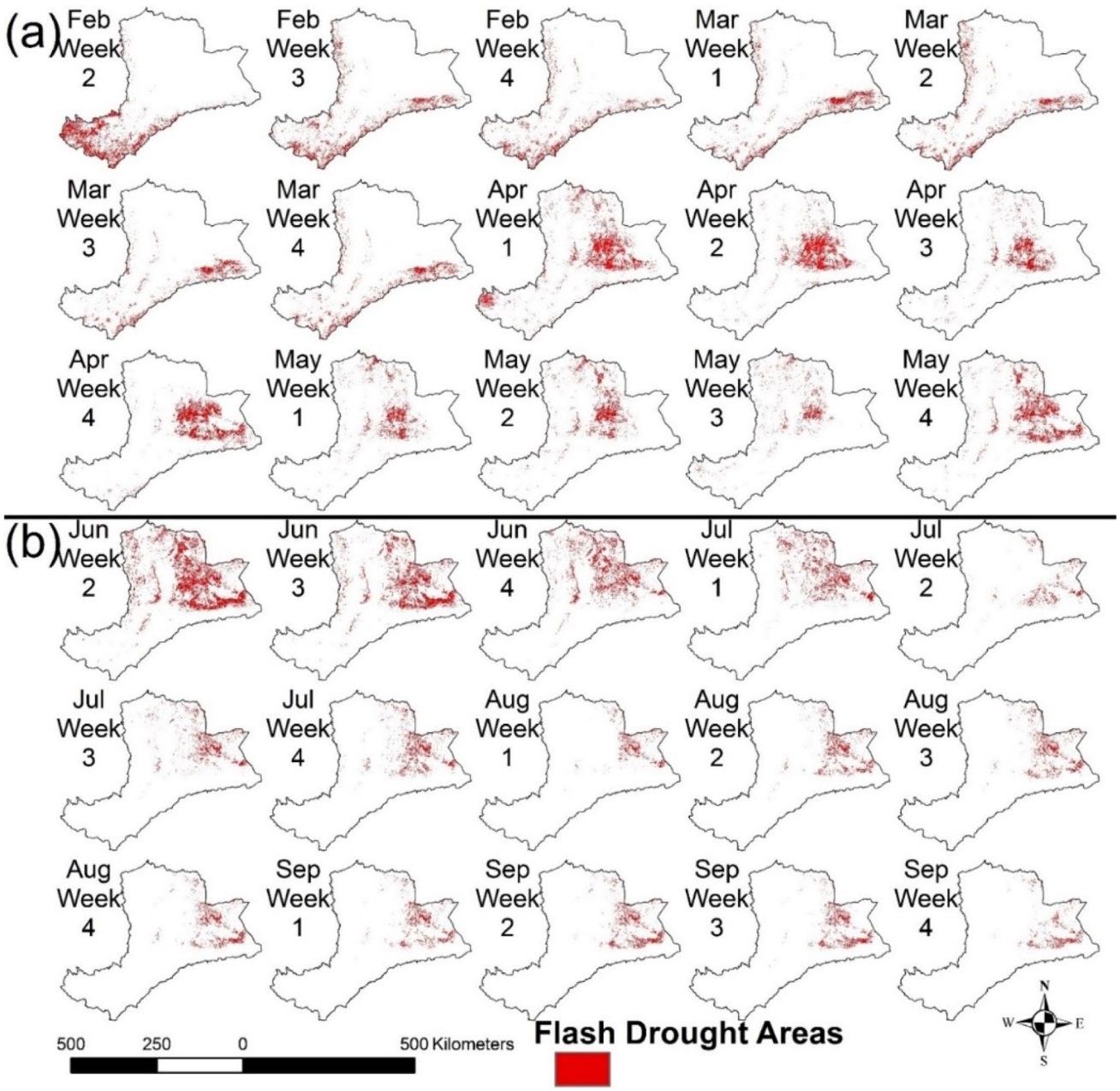

Figure 6 Spread of flash drought over the Awash River basin using weekly ESI in the case of 2008 historical drought: (: (**a**) during the mRS (February - May), and (**b**) during the MRS (June - September)

identified the mRS flash drought of 2008 began in the second week of February mainly over the upstream and southwestern basin. Starting from the third week of February till the fourth week of March, the flash drought expanded over the larger area of the basin, except for the downstream part of the basin. Similar to the ESI results, the EDDI flash drought shifted to the downstream basin during April and May, except for the first and second week of May. The area coverage of flash drought identified by the EDDI was larger than that by the ESI. As shown in Fig. 7b, the MRS flash drought was observed in the semi-arid part of the downstream basin. The MRS flash drought observed in the downstream basin was smaller in the first week of August and the first and second week of July as compared to those of the other weeks. Weekly flash drought identified by ESI and EDDI showed similar shifts in spatial distributions from one week to another, but their areal coverage was quite different from having larger flash drought areas by the EDDI.

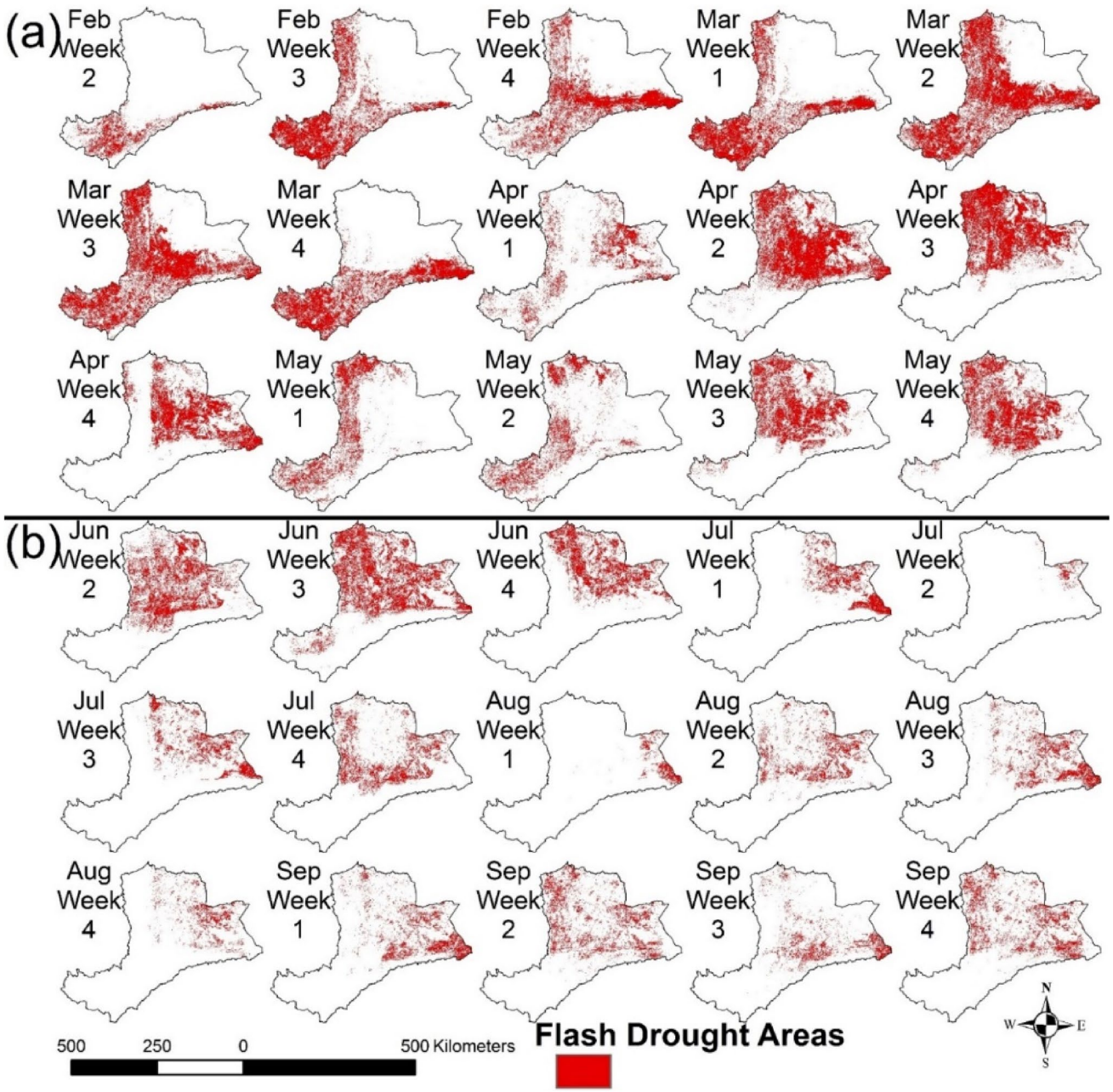

Figure 7 Spread of flash drought over the Awash River basin using weekly EDDI in the case of 2008 historical drought: during the mRS (February–May) (**a**) and during the MRS (June–September) (**b**)

3.3.3 Flash drought intensity based on ESI

Following the fourth criterion of flash drought given by Christian et al. (2019a, 2019b) that the mean changes in SSESI/ SEDDI must be below the 25th percentile for the entire pentads, it is able to indicate the rapid intensification of flash drought. As depicted in Fig. 8 and Table 3, the flash drought intensity was classified based on the mean changes in SSESI/SEDDI. Flash drought intensity was classified as an exceptional, extreme, severe, and moderate flash drought if the mean changes in SSESI/ SEDDI were respectively < 10th percentile, between 10th and 15th percentile, between 15th and 20th percentile, and between 20th and 25th percentile, respectively.

The ESI-based flash drought intensity of 2002, 2008, 2009, 2012, and 2015 droughts using the mean change in SSESI (< 25th percentile) were presented in Fig. 8 and Table 3. The exceptional and extreme flash drought intensity mainly exhibited in the highland and humid (i.e., upstream, southwestern, and northwestern) parts of the basin with

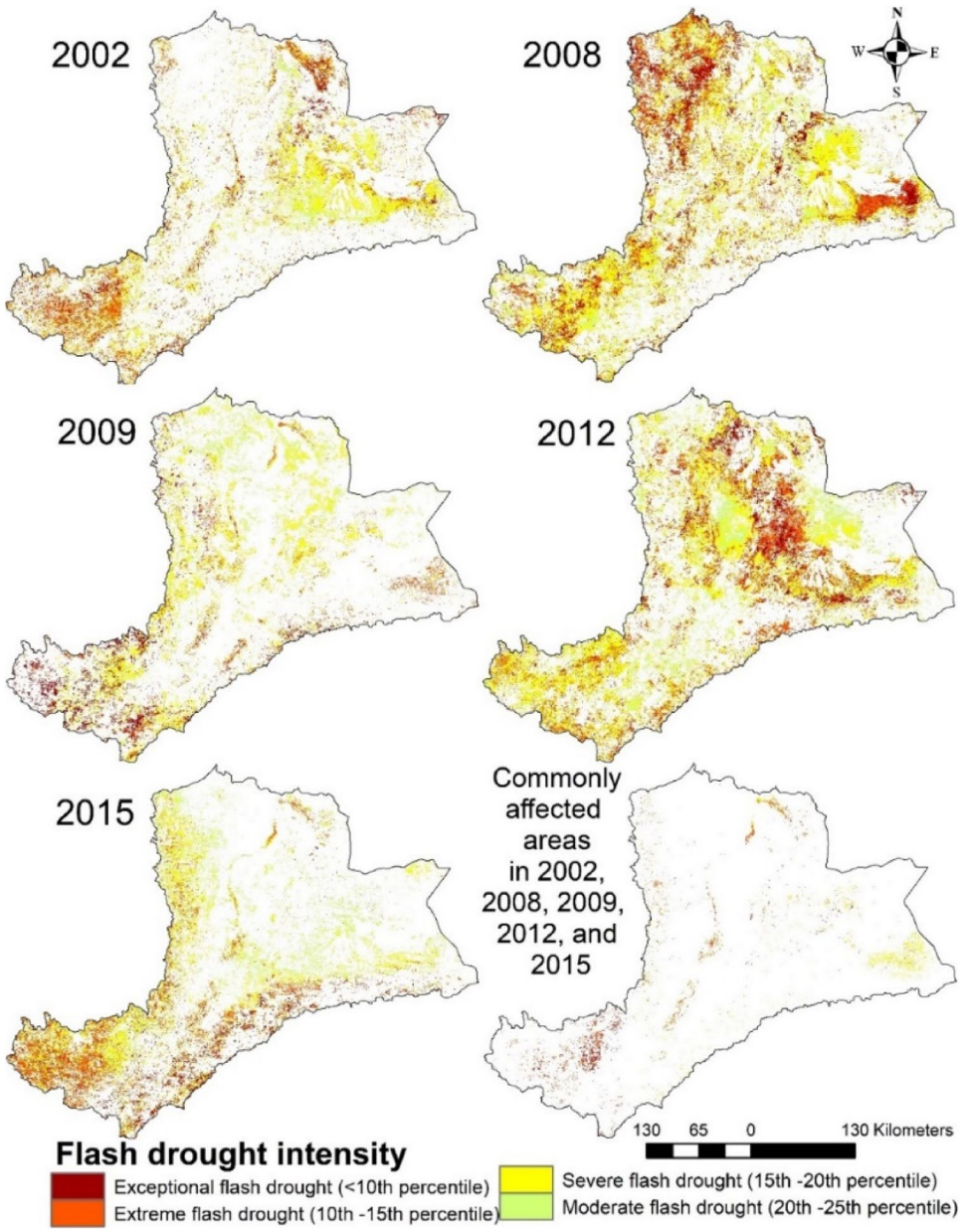

Figure 8 ESI-based flash drought intensity over the ARB using the mean changes in SSESI below the 25th percentile threshold in the case of 2002, 2008, 2009, 2012, and 2015 recent drought years

Table 3 ESI-based categories of flash drought intensity and their area (km^2) coverage in ARB in the cases of 2002, 2008, 2009, 2012, and 2015 recent drought years

Categories of flash drought intensity	Historical droughts years					Commonly affected areas
	2002	2008	2009	2012	2015	
Moderate flash drought	4423.5 (3.80%)	8663.8 (7.44%)	5427.6 (4.66%)	9960.4 (8.56%)	8391.4 (7.21%)	17.6 (0.02%)
Severe flash drought	11308.9 (9.72%)	19282.1 (16.57%)	10150.1 (8.72%)	19196.7 (16.50%)	9444.9 (8.12%)	1375 (1.18%)
Extreme flash drought	7942.2 (6.82%)	11792.1 (10.13%)	3792.7 (3.26%)	12003.1 (10.31%)	6827.3 (5.87%)	948 (0.81%)
Exceptional flash drought	2681.3 (2.30%)	6711.5 (5.77%)	3572.6 (3.07%)	4914.6 (4.22%)	2895.9 (2.49%)	14.4 (0.01%)
Total area	26355.9 (23%)	46449.5 (40%)	22943 (20%)	46074.8 (40%)	27559.5 (24%)	2355 (2%)

the most dominant land-cover types of agricultural crops, grasses, and shrublands. Additionally, the exceptional and extreme flash drought distribution observed in the lowland (i.e., downstream) part of the basin were directly linked to the rangelands (grasslands) of the area. The exceptional and extreme flash drought intensities in 2008 and 2012 extended over the ARB were larger than those of the other drought years. For example, the exceptional and the extreme flash drought covered 5.77 % (6711.5 km^2) and 10.13 % (11792.1 km^2), respectively, of the basin area in the 2008 drought (Table 2). The upstream (agricultural lands), irrigated croplands along the river, and the downstream (grasslands) part of the basin experienced a prevalence of flash drought. Overall, the area of the ARB that experienced flash drought in 2002, 2008, 2009, 2012, and 2015 are 23 % (26355.9 km^2), 40 % (46449.5 km^2), 20 % (22943 km^2), 40 % (46074.8km^2), and 24 % (27559.5 km^2), respectively.

3.3.4 Flash drought intensity based on EDDI

Figure 9 and Table 4 presented the EDDI-based flash drought intensity of 2002, 2008, 2009, 2012, and 2015. The results of EDDI are similar to those of ESI, except the areal extent of flash drought identified by EDDI was generally larger than that by the ESI. Similarly, agricultural and grassland areas were highly affected by flash drought. Overall, most of the basin experienced flash droughts with different intensities from one year to another. During 2002, the

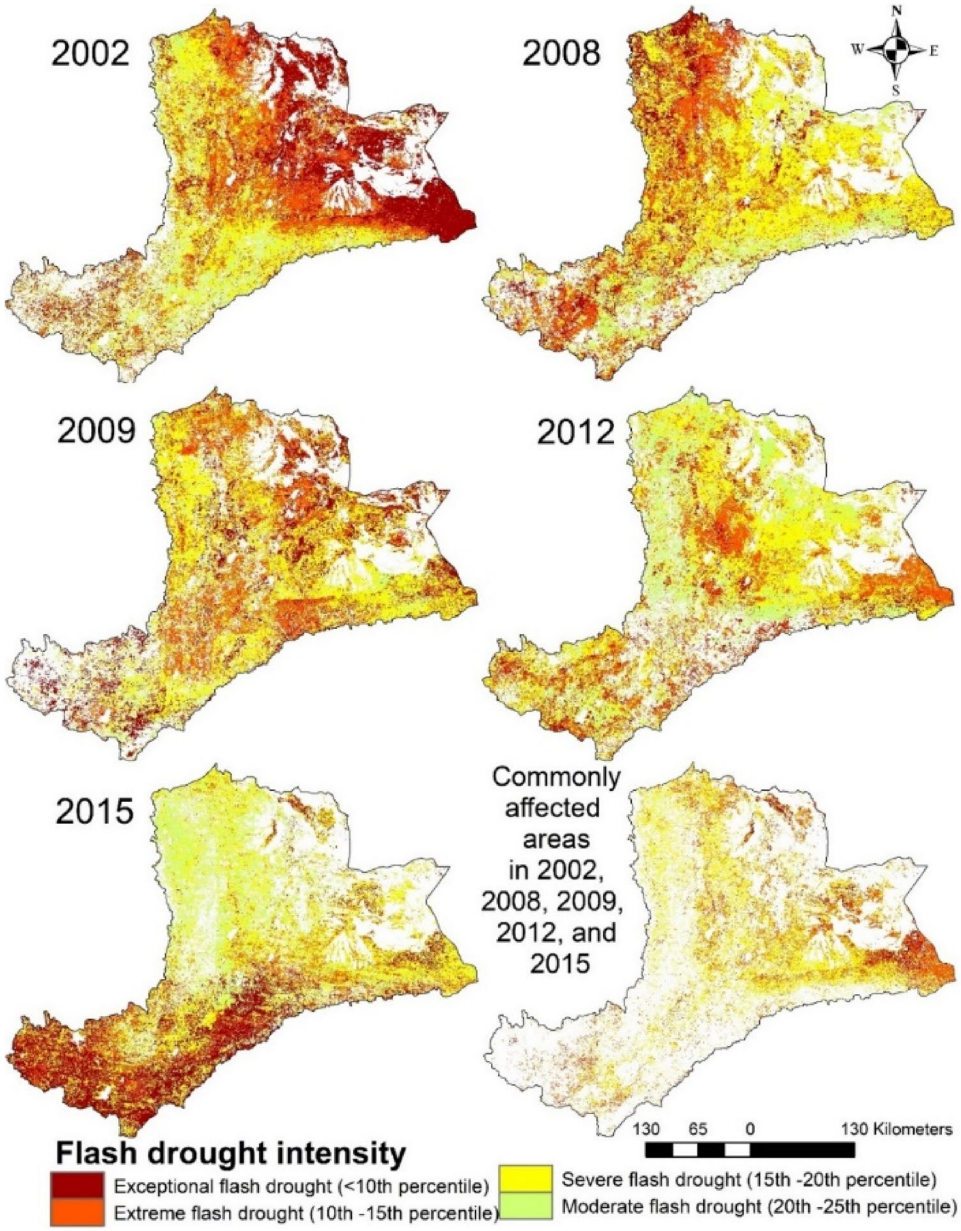

Figure 9 EDDI-based flash drought intensity over the ARB using the mean changes in SEDDI below the 25th percentile threshold in the case of 2002, 2008, 2009, 2012, and 2015 recent drought years

Table 4 EDDI-based categories of flash drought intensity and their area (km^2) coverage in ARB in the cases of 2002, 2008, 2009, 2012, and 2015 recent drought years

Flash drought intensity	Historical droughts years					Commonly affected areas
	2002	2008	2009	2012	2015	
Moderate flash drought	14558.8 (12.51%)	15151.9 (13.02%)	11315.7 (9.72%)	24346.2 (20.92%)	21118.9 (18.15%)	807.5 (0.69%)
Severe flash drought	20065.9 (17.24%)	34395.8 (29.56%)	29968.7 (25.75%)	28097.3 (24.14%)	27136.8 (23.32%)	21150.4 (18.17%)
Extreme flash drought	25657.1 (22.05%)	23009.3 (19.77%)	21228.9 (18.24%)	20569.9 (17.68%)	10464.6 (8.99%)	12592.8 (10.82%)
Exceptional flash drought	22758.3 (19.56%)	11285.2 (9.70%)	15026.3 (12.91%)	5696.8 (4.90%)	18765.9 (16.31%)	1285.5 (1.10%)
Total area	83040.1 (71.4%)	83842.2 (72.05%)	77539.6 (66.63%)	78710.2 (67.64%)	77486.2 (66.58%)	35836.2 (30.79%)

exceptional and extreme flash drought coverages were larger than those of other years and covered 19.56 % (22758.3 km^2) and 22.05% (25657.1 km^2) of the basin, respectively.

Several flash drought studies were conducted in the United States and they found that agricultural lands and grasslands were highly vulnerable to flash drought because

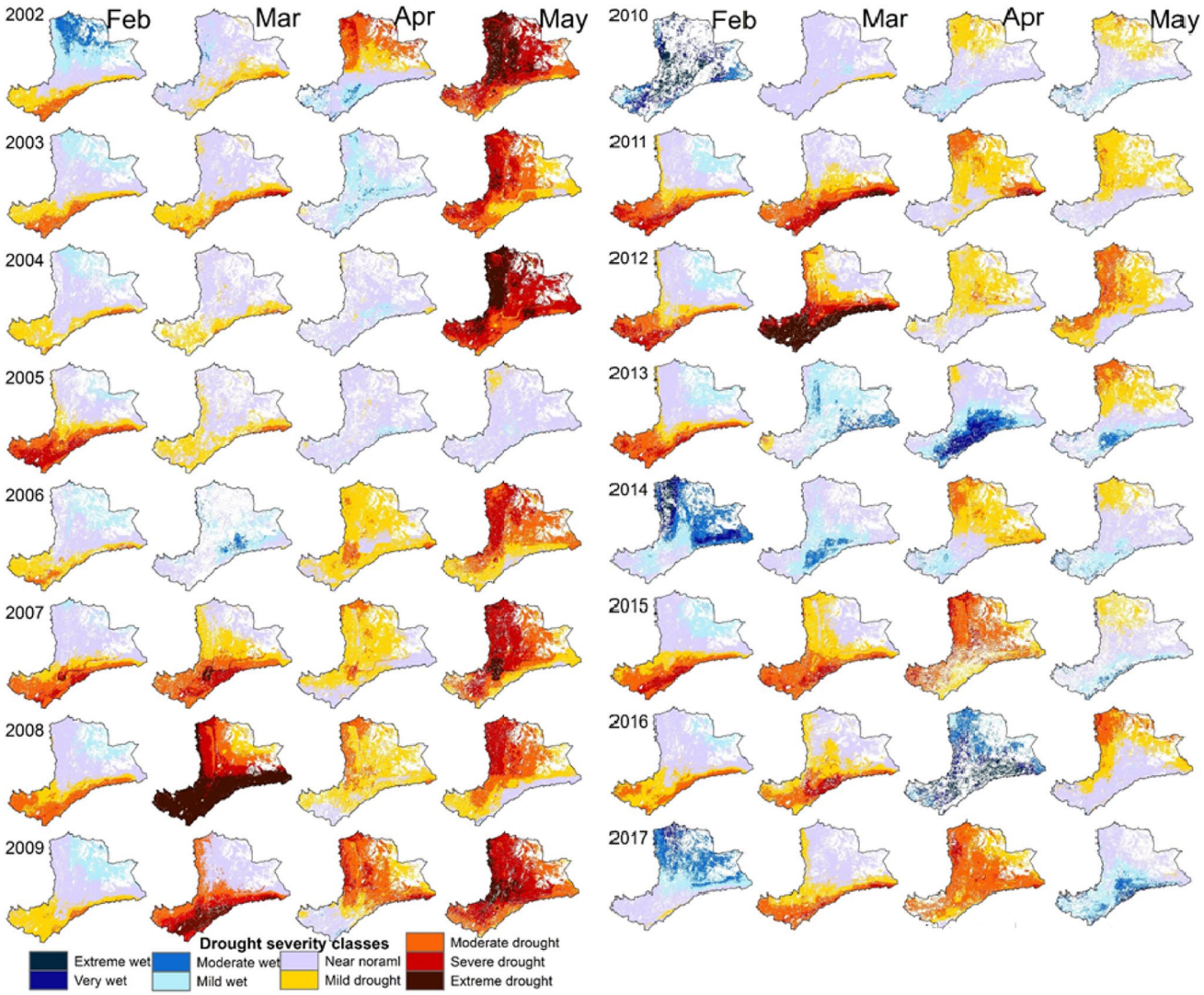

Figure 10 Monthly EDDI-based full-blown conventional drought in the mRS (2002–2017)

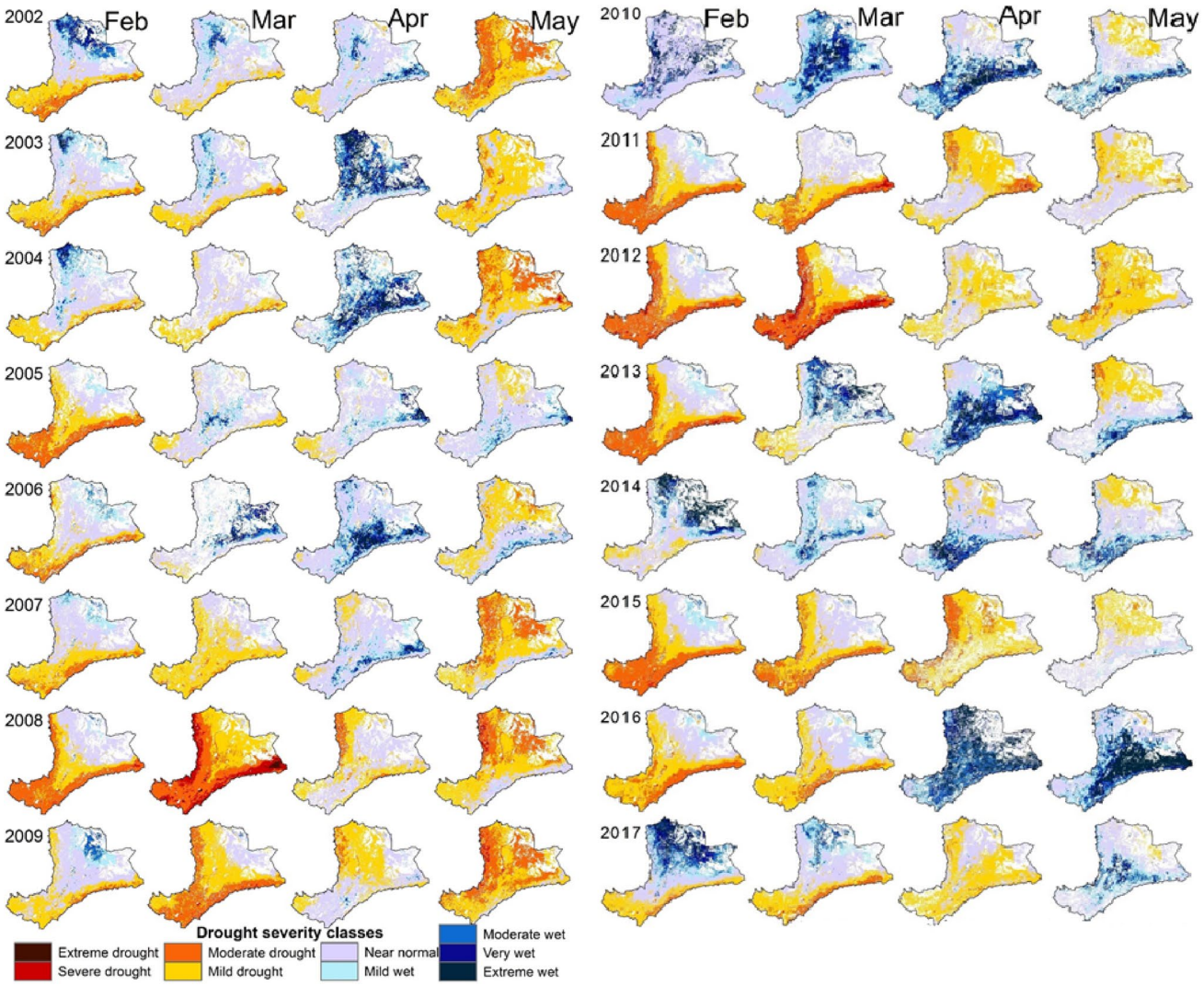

Figure 11 Monthly ESI-based full-blown conventional drought in the mRS (2002–2017)

of the shallow root system and high rate of evapotranspiration (Otkin et al. 2014; Mo and Lettenmaier 2016; Otkin et al. 2018; Christian et al. 2019a, 2019b). Moreover, comparatively agricultural lands were more prone to flash drought than grasslands. Our results generally agreed with their findings, the ARB were highly vulnerable to flash drought over upstream agricultural land, irrigation cropland along the river, and downstream grasslands. High temperatures and densely vegetated areas were also exposed to flash drought risks due to the increase in evapotranspiration from the vegetation (Zhang et al. 2019). Semiarid plain regions are sensitive to land-atmosphere interaction, such as the decreased evapotranspiration caused by reduced soil moisture will limit the local source of boundary layer moisture to restrict atmospheric moisture advection. As a result, the atmosphere remains dry to increase the evaporative demand and the dry soil keeps altering the ambient environment to be less supportive of convective rainfall and intensifies flash drought (Basara and Christian 2018; Christian et al. 2019a, 2019b). They also reported that regions that lack soil water availability and have sparse vegetation could not be susceptible to flash drought.

EDDI is mostly vital for flash drought early warning because it is independent of rainfall and soil moisture with less uncertainty related to topography and regional convective activities (Hobbins et al. 2016). EDDI is also sensitive to two distinct land-surface atmosphere interactions (Hobbins et al. 2016; McEvoy et al. 2016): (1) The surface moisture limitation that leads to declining of ET and increasing of PET indicates a sustained drought, and (2) the increases of ET and PET from increased energy availability that results in surface moisture limitation to trigger a flash drought. PET can rise in all drought cases and could be the first sign of drought (Hobbins et al. 2016). The flash

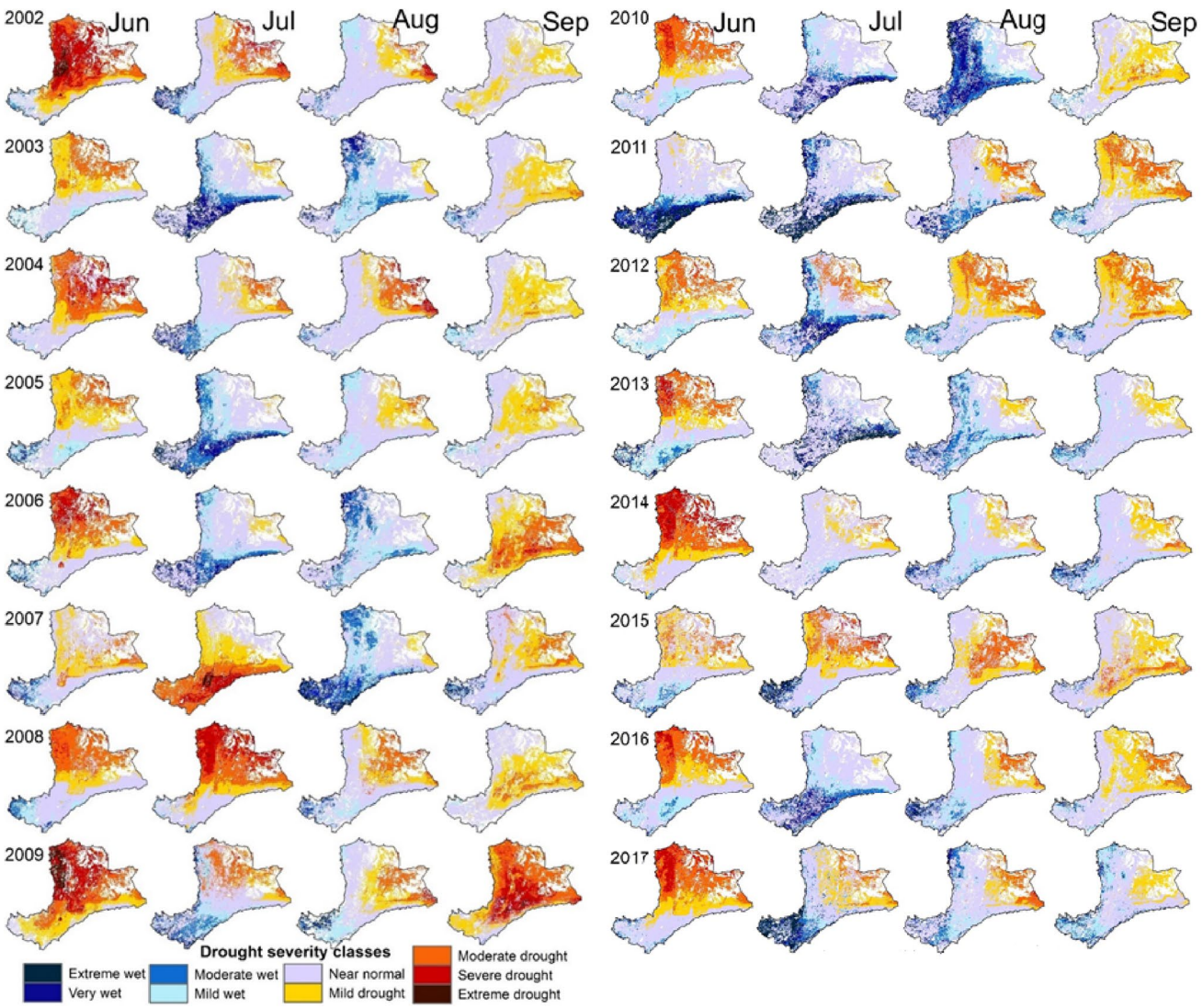

Figure 12 Monthly EDDI-based full-blown conventional drought in the MRS (2002–2017)

drought extent under EDDI is larger as compared to ESI in the ARB because of the first condition that under a water-limited environment, ET and PET respond in the opposite direction, which indicates a sustained drought.

3.4 Conventional drought using ESI and EDDI from 2002 to 2017

In addition to the weekly analysis of the flash drought, the conventional drought from 2002 to 2017 was looked at to see whether the flash drought progresses to a full-blown conventional drought or not. The majority of the evaluated flash drought episodes, including 2002, 2008, 2009, 2012, and 2015, were extended to conventional drought regardless of the number of dry months and the magnitude of the drought, as shown in Figs. 10, 11, 12, 13, and 14. The month of May exhibited more frequent drought as compared to other months of the mRS (i.e., February, March April, and May) as shown in Figs. 10 and 11. Similar to the flash drought results, the spatial extent and severity of conventional drought identified by the EDDI were much greater than those by the ESI. For example, the spatial pattern of conventional drought was similar to those of flash drought identified in February and March, mainly over the upstream (southwest) and peripheries of the basin. In the month of April and May, almost the entire and north-eastern (downstream) part of the basin experienced more drought compared to other parts of the basin.

The month of June exhibited more frequent drought followed by September than those of other months in the MRS (i.e., June, July, August, and September) as shown in Figs. 12 and 13. The conventional drought pattern in the

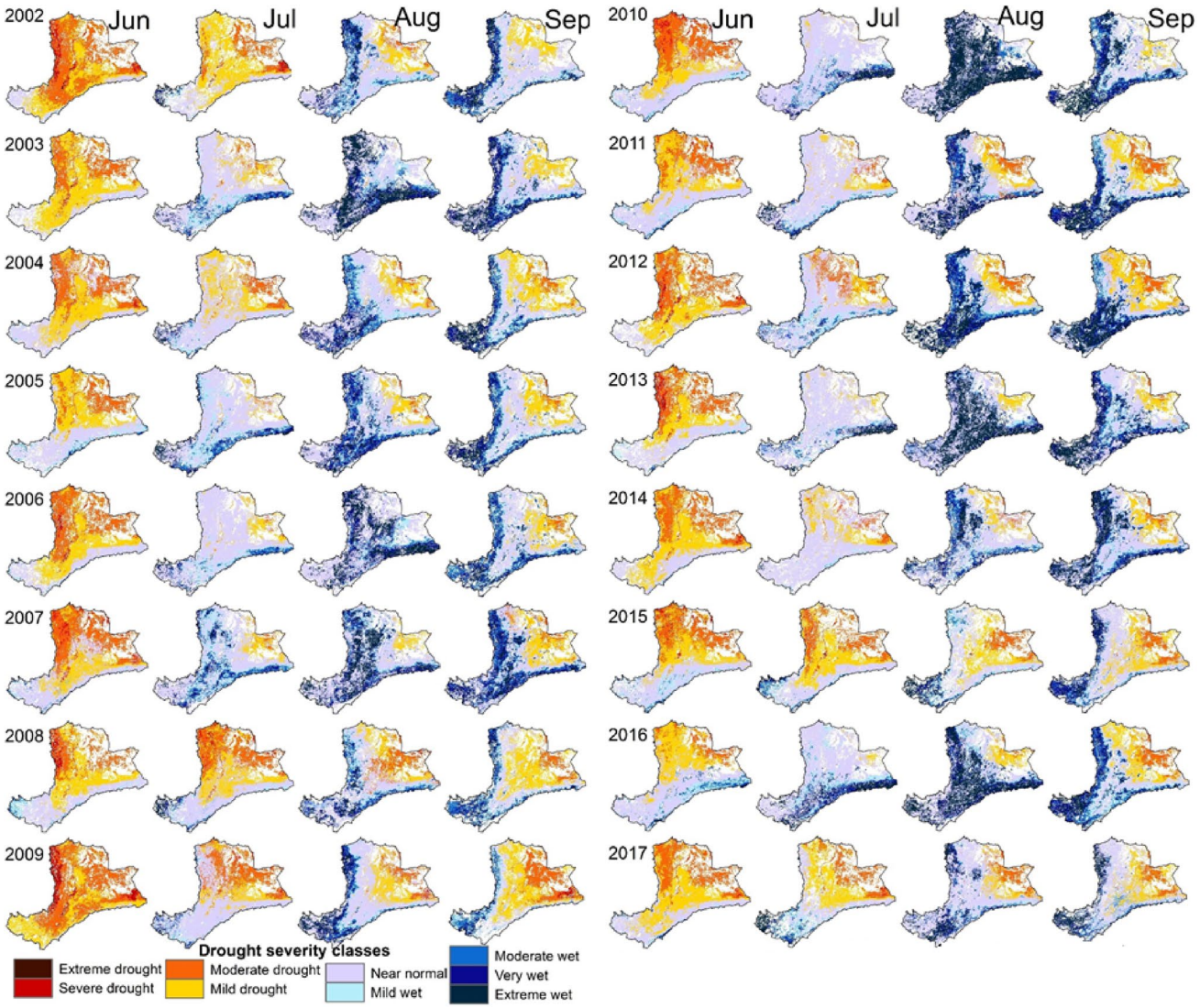

Figure 13 Monthly ESI-based full-blown conventional drought in the MRS (2002–2017)

MRS is similar to the results of flash drought in that the north-eastern (downstream) part of the basin experienced more drought during July, August, and September, whereas in June the entire basin exposed more drought.

4 Conclusions

The most severe droughts in recent years over the ARB were evaluated with the flash drought indices and approaches proposed by Christian et al. (2019a, 2019b). The distributions of flash drought during the mRS and the MRS in 2008 were identified with both EDDI and ESI. Flash droughts that rapidly intensify within a week were also examined. Mostly observed in February and March, the upstream, northwestern, and southwestern peripheries of the ARB experienced flash drought in 2008 with the spatial coverages mainly correlated with agricultural crops and grasslands. During April and May, the flash drought in the upstream basin became less and expanded to the downstream, particularly the northeastern and southeastern basins. During most weeks of the MRS, the downstream basin was identified to experience flash drought. Since the EDDI is solely dependent on PET and it can intensify with increasing temperature regardless of rainfall and soil moisture, the flash drought extent identified by the EDDI was generally larger than that by the ESI. Based on different drought intensities, flash droughts were classified as exceptional, extreme, severe, and moderate flash droughts. The exceptional and extreme flash droughts mainly exhibited in the highland and humid (i.e., upstream, southwestern, and northwestern) parts of the basin with dominant

land-use types of agricultural crops, grass, and shrublands. Additionally, exceptional and extreme flash droughts were found in the lowland downstream part of the basin with grasslands as the dominant land-use types. The irrigated croplands along the river were also identified to be highly vulnerable to flash drought. Similar to the weekly flash drought, the monthly full-blown conventional drought analysis showed that the majority of historical drought occurrences occurred during the month of June during the main rainy season, whereas the majority of such events were seen during the months of April and May during the minor rainy season. Early identification of flash drought expansion based on AET and PET under rising temperatures will be very helpful for developing drought monitoring. Particularly the EDDI is more sensitive to warming temperatures having the advantage of detecting the early onset of flash drought, which is vital for developing drought early warning. Using a shorter time resolution, the flash drought analysis can detect the early onset of drought as compared to the conventional drought analysis with a longer time resolution. By incorporating flash drought, evaluations into drought monitoring and early warning will be very helpful to enhance proactive risk management strategies, minimize potential losses of agricultural production, and increase food security.

5 Recommendation and future direction

The lack of adequate and reliable observed data was the main challenge in this study. The meteorological stations are sparse especially in the downstream part of the ARB and without having long-term observed data. Thus, increasing the density of meteorological stations would be helpful for future drought evaluation and monitoring in the basin, especially over areas vulnerable to flash drought. For areas with rapid intensification of flash drought, it is recommended to deploy instruments to support the analysis of flash drought with daily soil moisture, rainfall, and temperature data. Soil moisture evaluation at different depths in response to EDDI and ESI indices will enhance early detectability of flash drought that improves drought monitoring and predictions. Further investigations are suggested to understand the effects of different land-use and land-cover types on the onset and evolution of flash drought and the interactions between them. Examining flash drought response in relation to the ENSO and extreme events and incorporating climate projections to assess climate change impacts will be more important for minimizing the drought risk in the basin.

Acknowledgements We greatly recognized the groups producing MODIS datasets in the National Aeronautics and Space Administration (NASA) and the United States Geological Survey (USGS). We also acknowledged the Ethiopian Meteorology Institute for giving us the observed meteorological datasets. Many thanks to Dr. Pratul Ranjan Karn for his valuable time to edit the manuscript for proper English language.

Author contribution Yitea Seneshaw Getahun: process and analysis the data, data interpretation, and drafting of the first version of the manuscript. Ming-Hsu Li: revised the paper and amended the manuscript.

Declarations

Competing interests The authors declare no competing interests.

References

Adeba D, Kansal ML, Sen S (2015) Assessment of water scarcity and its impacts on sustainable development in Awash basin, Ethiopia. Sustain Water Resour Manag 1(1):71–87. https://doi.org/10.1007/s40899-015-0006-7

AghaKouchak A, Farahmand A, Melton FS, Teixeira J, Anderson MC, Wardlow BD, Hain CR (2015) Remote sensing of drought: progress, challenges and opportunities. Rev Geophys 53:452–480, Blackwell Publishing Ltd. https://doi.org/10.1002/2014RG000456

Anderson MC, Hain C, Wardlow B, Pimstein A, Mecikalski JR, Kustas WP (2011) evaluation of drought indices based on thermal remote sensing of evapotranspiration over the continental United States. J Clim 24(8):2025–2044. https://doi.org/10.1175/2010JCLI3812.1

Anderson MC, Zolin CA, Sentelhas PC, Hain CR, Semmens K, Tugrul Yilmaz M, Tetrault R (2016) The Evaporative Stress Index as an indicator of agricultural drought in Brazil: an assessment based on crop yield impacts. Remote Sens Environ 174:82–99. https://doi.org/10.1016/j.rse.2015.11.034

Basara JB, Christian JI (2018) Seasonal and interannual variability of land-atmosphere coupling across the Southern Great Plains of North America using the North American regional reanalysis. Int J Climatol 38:964–978. https://doi.org/10.1002/joc.5223

Christian JI, Basara JB, Otkin JA, Hunt ED (2019b) Regional characteristics of flash droughts across the United States. Environ Res Commun 1(12):125004. https://doi.org/10.1088/2515-7620/AB50CA

Christian JI, Basara JB, Otkin JA, Hunt ED, Wakefield RA, Flanagan PX, Xiao X (2019a) A methodology for flash drought identification: application of flash drought frequency across the United States. J Hydrometeorol 20(5):833–846. https://doi.org/10.1175/JHM-D-18-0198.1

Degefu MA, Rowell DP, Bewket W (2017) Teleconnections between Ethiopian rainfall variability and global SSTs: observations and methods for model evaluation. Meteorog Atmos Phys 129(2):173–186. https://doi.org/10.1007/s00703-016-0466-9

Dost, R, Obando EB, Hoogeveen W (2013) Water Accounting Plus (WA+) in the Awash River Basin Coping with Water Scarcity-Developing National Water Audits Africa Client: FAO, Land and Water Division. http://www.wateraccounting.org/files/projects/awash_basin.pdf. Accessed on 15 Juy 2020

Edossa DC, Babel MS, DasGupta A (2010) Drought analysis in the Awash River Basin, Ethiopia. Water Resour Manag 24(7):1441–1460. https://doi.org/10.1007/s11269-009-9508-0

El Kenawy AM, McCabe MF, Vicente-Serrano SM, López-Moreno JI, Robaa SM (2016) Changes in the frequency and severity of hydrological droughts over Ethiopia from 1960 to 2013. Cuad de Investig Geogr 42:145–166. https://doi.org/10.18172/cig.2931

Farahmand A (2016) Frameworks for improving multi-index drought monitoring using remote sensing observations. Ph.D. Theses and Dissertations, UC Irvine, USA. Available online https://escholarship.org/uc/item/5x29g304. Accessed May 15, 2020

Ford TW, Labosier CF (2017) Meteorological conditions associated with the onset of flash drought in the eastern United States. Agric For Meteorol 247:414–423 https://agris.fao.org/agris-search/search.do?recordID=US201800046670. Accessed 2023-02-04

Ford TW, McRoberts DB, Quiring SM, Hall RE (2015) on the utility of in situ soil moisture observations for flash drought early warning in Oklahoma, USA. Geophys Res Lett 42(22):9790–9798. https://doi.org/10.1002/2015GL066600

Gebissa B, Geremew W (2022) Determinants of food insecurity and the choice of livelihood strategies: the case of Abay chomen district, Oromia regional state, Ethiopia. Sci World J 2022:1–15. https://doi.org/10.1155/2022/1316409

Gebremeskel G, Tang Q, Sun S, Huang Z, Zhang X, Liu X (2019) Droughts in East Africa: causes, impacts and resilience. Earth Sci Rev 193:146–161. Elsevier B.V. https://doi.org/10.1016/j.earscirev.2019.04.015

Hailu R, Tolossa D, Alemu G (2017) Water security: stakeholders' arena in the Awash River Basin of Ethiopia. Sustain Water Resour Manag 1:19. https://doi.org/10.1007/s40899-017-0208-2

Hobbins MT, Wood A, McEvoy DJ, Huntington JL, Morton C, Anderson M, Hain C (2016) the Evaporative Demand Drought Index. Part I: Linking Drought Evolution to Variations in Evaporative Demand. J Hydrometeorol 17(6):1745–1761. https://doi.org/10.1175/JHM-D-15-0121.1

Liou Y-A, Mulualem GM (2019) Spatio–temporal assessment of drought in ethiopia and the impact of recent intense droughts. Remote Sens 11(15):1828. https://doi.org/10.3390/rs11151828

MacDonald AM, Bell RA, Kebede S, Azagegn T, Yehualaeshet T, Pichon F, Calow RC (2019) Groundwater and resilience to drought in the Ethiopian highlands. Environ Res Lett 14(9):095003. https://doi.org/10.1088/1748-9326/ab282f

Masih I, Maskey S, Mussá FE, Trambauer P (2014) A review of droughts on the African continent: a geospatial and long-term perspective. Hydrol Earth Syst Sci 18(9):3635–3649. https://doi.org/10.5194/hess-18-3635-2014

Mays L (2014) Integrated urban water management: arid and semi-arid regions. In: Integrated Urban Water Management: Arid and Semi-Arid Regions. CRC Press. https://doi.org/10.1201/9781482266207

McEvoy DJ, Hobbins M, Brown T, VanderMolen K, Wall T, Huntington J, Svoboda M (2019) Establishing Relationships between drought indices and wildfire danger outputs: a test case for the California-Nevada drought early warning system. Climate 7(4):52. https://doi.org/10.3390/cli7040052

McEvoy DJ, Huntington JL, Hobbins MT, Wood A, Morton C, Anderson M, Hain C (2016) The evaporative demand drought index. Part II: CONUS-Wide Assessment against Common Drought Indicators. J Hydrometeorol 17(6):1763–1779. https://doi.org/10.1175/JHM-D-15-0122.1

McKee TB, Doesken NJ, Kleist J (1993) The relationship of drought frequency and duration to time scales. http://citeseerx.ist.psu.edu/viewdoc/summary?doi=10.1.1.462.4342. Accessed 2022-09-12

Mera GA (2018) Drought and its impacts in Ethiopia. In: Weather and Climate Extremes. Elsevier B.V. https://doi.org/10.1016/j.wace.2018.10.002

Mo KC, Lettenmaier DP (2016) Precipitation Deficit Flash Droughts over the United States. J Hydrometeorol 17(4):1169–1184. https://doi.org/10.1175/JHM-D-15-0158.1

Mohammed Y, Yimer F, Tadesse M, Tesfaye K (2017) Meteorological drought assessment in northeast highlands of Ethiopia. https://doi.org/10.1108/IJCCSM-12-2016-0179

Mu Q, Heinsch FA, Zhao M, Running SW (2007) Development of a global evapotranspiration algorithm based on MODIS and global meteorology data. Remote Sens Environ 111(4):519–536. https://doi.org/10.1016/j.rse.2007.04.015

Mu Q, Zhao M, Running SW (2011) Improvements to a MODIS global terrestrial evapotranspiration algorithm. Remote Sens Environ 115(8):1781–1800. https://doi.org/10.1016/j.rse.2011.02.019

Munagapati H, Yadav R, Tiwari VM (2018) Identifying water storage variation in Krishna Basin, India from in situ and satellite based hydrological data. J Geol Soc India 92(5):607–615. https://doi.org/10.1007/s12594-018-1074-8

Murendo C, Keil A, Zeller M (2010) Drought impacts and related risk management by smallholder farmers in developing countries: evidence from Awash River Basin, Ethiopia. Research in Development Economics and Policy https://ideas.repec.org/p/ags/uhohdp/114750.html. Accessed 2022-08-12

Otkin JA, Anderson MC, Hain C, Svoboda M (2014) Examining the relationship between drought development and rapid changes in the evaporative stress index. J Hydrometeorol 15(3):938–956. https://doi.org/10.1175/JHM-D-13-0110.1

Otkin JA, Svoboda M, Hunt ED, Ford TW, Anderson MC, Hain C, Basara JB (2018) Flash droughts: a review and assessment of the challenges imposed by rapid-onset droughts in the United States. Bull Am Meteorol Soc 99(5):911–919. https://doi.org/10.1175/BAMS-D-17-0149.1

Pendergrass AG, Meehl GA, Pulwarty R, Hobbins M, Hoell A, AghaKouchak A, Bonfils CJW, Gallant AJE, Hoerling M, Hoffmann D (2020) Flash droughts present a new challenge for subseasonal-to-seasonal prediction. Nat Clim Chang 10:191–199. https://doi.org/10.1038/s41558-020-0709-0

Priestley CHB, Taylor RJ (1972) On the assessment of surface heat flux and evaporation using large-scale parameters. Mon Weather Rev 100:81–92. https://doi.org/10.1175/1520-0493(1972)100%3C0081:otaosh%3E2.3.co;2

Running SW, Mu Q, Zhao M (2017a) MOD16A2: MODIS/Terra Net Evapotranspiration 8-Day L4 Global 500 m SIN Grid V006. Distributed by NASA EOSDIS Land Processes DAAC. https://lpdaac.usgs.gov/products/mod16a2v006/. Accessed on 2020-02-12

Running SW, Mu Q, Zhao M, Moreno A (2017b) User's Guide MODIS Global Terrestrial Evapotranspiration (ET) Product (NASA MOD16A2/A3) NASA Earth Observing System MODIS Land Algorithm. https://ladsweb.modaps.eosdis.nasa.gov/missions-and-measurements/modis/MOD16_ET_User-Guide_2017.pdf. Accessed 2020-02-13

Shiferaw B, Tesfaye K, Kassie M, Abate T, Prasanna BM, Menkir A (2014) Managing vulnerability to drought and enhancing livelihood resilience in sub-Saharan Africa: technological, institutional and policy options. Weather Clim Extremes 3:67–79. https://doi.org/10.1016/j.wace.2014.04.004

Sun Z, Zhu X, Pan Y, Zhang J, Liu X (2018) Drought evaluation using the GRACE terrestrial water storage deficit over the Yangtze River Basin, China. Sci Total Environ 634:727–738. https://doi.org/10.1016/j.scitotenv.2018.03.292

Sur C, Hur J, Kim K, Choi W, Choi M (2015) An evaluation of satellite-based drought indices on a regional scale. Int J Remote Sens

36(22):5593–5612. https://doi.org/10.1080/01431161.2015.1101653
Suryabhagavan KV (2017) GIS-based climate variability and drought characterization in Ethiopia over three decades. Weather Clim Extremes 15:11–23. https://doi.org/10.1016/j.wace.2016.11.005
Svoboda M, LeComte D, Hayes M, Heim R, Gleason K, Angel J, Stephens S (2002) The Drought monitors. Bull Am Meteorol Soc 83(8):1181–1190. https://doi.org/10.1175/1520-0477-83.8.1181
Teweldebirhan TD, Uddameri V, Forghanparast F, Hernandez EA, Ekwaro-Osire S (2019) Comparison of Meteorological and Agriculture-Related Drought Indicators across Ethiopia. Water 11(11):2218. https://doi.org/10.3390/w11112218
Thomas EA, Needoba J, Kaberia D, Butterworth J, Adams EC, Oduor P, Nagel C (2019) Quantifying increased groundwater demand from prolonged drought in the East African Rift Valley. Sci Total Environ 666:1265–1272. https://doi.org/10.1016/j.scitotenv.2019.02.206
USAID (2018) The United States Agency for International Development. Economics of resilience to drought Ethiopia analysis. https://www.agrilinks.org/sites/default/files/ethiopia_economics_of_resilience_final_jan_4_2018_-_branded.pdf . Accessed July 11, 2020
Van Loon AF (2015) Hydrological drought explained. WIREs Water 2(4):359–392. https://doi.org/10.1002/wat2.1085
Vicente-Serrano SM, Beguería S, López-Moreno JI (2010) A Multiscalar Drought Index Sensitive to Global Warming: The Standardized Precipitation Evapotranspiration Index. J Clim 23(7):1696–1718. https://doi.org/10.1175/2009JCLI2909.1
Viste E (2012) Moisture Transport and Precipitation in Ethiopia. https://folk.uib.no/evi003/Publications/Viste_PhDthesis2012.pdf. Accessed 2023-01-12
Viste E, Sorteberg A (2013) Moisture transport into the Ethiopian highlands. Int J Climatol 33(1):249–263. https://doi.org/10.1002/joc.3409
Wilhite D (2002) Combating drought through preparedness. In: Natural resources forum (Vol. 26, No. 4, pp. 275-285). Blackwell Publishing Ltd., Oxford, UK and Boston, USA https://onlinelibrary.wiley.com/doi/abs/10.1111/1477-8947.00030. Accessed 2022-10-12
Wilhite D, Pulwarty RS (2017) Drought and water crises: integrating science, management, and policy. CRC Press
World Bank (2017) Federal Democratic Republic of Ethiopia, Rural Productive Safety Net Project (P163438). http://documents1.worldbank.org/curated/en/830381505613638420/pdf/project-appraisal-document-pad-P163438-EU-edits-for-Board-version-08252017.pdf. Accessed July 11, 2020
Yao N, Li Y, Lei T, Peng L (2018) Drought evolution, severity and trends in mainland China over 1961–2013. Sci Total Environ 616–617:73–89. https://doi.org/10.1016/j.scitotenv.2017.10.327
Yu W, Li Y, Cao Y, Schillerberg T (2019) Drought Assessment using GRACE Terrestrial Water Storage Deficit in Mongolia from 2002 to 2017. Water 11(6):1301. https://doi.org/10.3390/w11061301
Zeleke TT, Giorgi F, Diro GT, Zaitchik BF (2017) Trend and periodicity of drought over Ethiopia. Int J Climatol 37(13):4733–4748. https://doi.org/10.1002/joc.5122
Zhang X, Li M, Ma Z, Yang Q, Lv M, Clark R (2019) Assessment of an evapotranspiration deficit drought index in relation to impacts on ecosystems. Adv Atmos Sci 36(11):1273–1287. https://doi.org/10.1007/s00376-019-9061-6